



Shahrood University of
Technology



Iranian Society of
Mining Engineering
(IRSM)

Investigating the Influence of Sample Geometric Variations on Mechanical Characterization in Rock and Concrete

Amirhossein Naseri¹, Behnam Maleki², Tohid Asheghi Mehmandari², Amin Tohidi³, and Ahmad Fahimifar^{2*}

1. Faculty of Garmsar, Amirkabir University of Technology, Tehran, Iran

2. Faculty of Civil and Environmental Engineering, Amirkabir University of Technology, Tehran, Iran

3. Faculty of Mining Engineering, Amirkabir University of Technology, Tehran, Iran

Article Info

Received 4 June 2024

Received in Revised form 4 July 2024

Accepted 4 August 2024

Published online 4 August 2024

DOI: [10.22044/jme.2024.14631.2759](https://doi.org/10.22044/jme.2024.14631.2759)

Keywords

Shape and size effect

Uniaxial compressive strength

Elastic modulus

Pressure wave velocity

Heterogeneity

Abstract

The present study delves into investigating the impact of sample size and geometry on the mechanical behavior of rock and concrete. More specifically, it examines factors including Uniaxial Compressive Strength (UCS), Elastic Modulus (E), and Pressure Wave Velocity (V_p). Results indicated a notable correlation between the dimensions and morphology of the specimens with these properties. All tests were conducted at a uniform loading rate of 0.002 mm/s. According to the outcomes, the effect of sample size and shape on UCS for concrete is more predictable than for rock. The increase in the sample size led to an initial increase followed by a decline in the UCS values of the rocks. Furthermore, the concrete typically showed a drop in the UCS values as sample size increased. The UCS and E values rose at first before falling, suggesting the existence of a sample size with maximum UCS. The V_p values of the prismatic rock and concrete samples continually grew. After attaining their optimum strength, the prismatic samples showed greater degrees of flexibility and ductility compared to cylindrical ones because of post peak behavior. This suggests that prismatic samples, with their less slender geometry and reduced tendency for brittle behavior, are deemed more suitable for UCS testing. These results can improve the accuracy of assessing the mechanical properties of tunneling materials, particularly those used in subsurface construction in urban roads and highways.

Notation List

UCS	Uniaxial compressive strength, (MPa)
A	Sample Cross-sectional area, (mm ²)
d	Sample diameter, (mm)
E	Elastic modulus, (GPa)
F _{value}	Obtained statistic
h	Sample height, (mm)
L	Sample length, (mm)
MD	Mean difference is a subtraction of J group mean from I
NS	Normalized slope
P _{max}	Maximum load, (N)
p-value	Defined as the probability assuming no effect or difference occurs
SE	Standard error of the mean for each size being compared
t	Wave emission and reception time, (s)
V _p	Pressure wave velocity, (m/s)
w	Sample width, (mm)
σ	Stress, (MPa)
ε	Strain (%)

1. Introduction

For designing and constructing structures on or in rock and using concrete as a support of tunnels the need to experiment to find the behavior of rock and concrete is vital. However, the size and shape effect of samples can affect the results. For size effect, the ISRM and ASTM recommends cylindrical samples $\frac{L}{D} \approx 2-3$, because of lower $\frac{L}{D}$ the shear failure mode cannot take place and for higher $\frac{L}{D}$ the buckling failure happened that can mislead the designers. The important note for sample with the same $\frac{L}{D}$ ratios, by increasing the size the probability of occurrence heterogeneity and anisotropy increased. So, in this paper by

✉ Corresponding author: fahim@aut.ac.ir (A. Fahimifar)

conducting some experiments the size effect of rock and concrete were examined precisely.

The reason for the different shape effect impact on UCS parameter comes back to stress concentration; in cylindrical samples the uniform stress distribution than in cubic samples. Because in cubic samples stress concentration at corners can affect the results. So, converting the UCS results from cubic into cylindrical samples may be inappropriate. Thus, this paper studies both the size and shape effect of the samples with an experimental approach.

Previous studies have consistently classified rocks and their man-made equivalents, such as concrete, as materials exhibiting brittleness and quasi-brittleness. This categorization is primarily based on their mechanical response, which is defined by parameters like Uniaxial Compressive Strength (UCS) and Elastic Modulus (E). The assessment of UCS can be carried out non-destructively using methods like pressure wave velocity (V_p) testing, offering valuable insights while preserving the original state of the samples.

The parameter known as UCS plays a critical role in designing materials for various assessments, including fatigue, triaxial compressive strength, and Hopkinson dynamic tests. This implies that materials exhibiting higher UCS levels demonstrate superior ability to withstand dynamic and cyclic loading and enhanced durability against weathering and chemical reaction.

This test measures the fundamental mechanical characteristics of rocks such as peak strength, pre peak stress strain curve, and failure plane which are affected by multiple variables such as the sample size and shape, as well as the rock texture and structure. It is an important indicator for the overall mechanical assessment of geological materials [1-6].

The size effect is an important factor in determining UCS values of rock and concrete. Therefore, the length-to-diameter ratio of a sample emerges as a critical metric reflecting the size effects on samples. Experimental findings delineate a clear relationship between this ratio and the materials' UCS, with a trend where a decrease in the length-to-diameter ratio corresponds to an increase in the UCS values of rock and concrete [7-15]. Accordingly, it is crucial to develop a standardized ratio for the precise and consistent measurement of UCS. The American Society for Testing and Materials (ASTM) suggests a prescribed length-to-diameter ratio of 2 to 2.5 [16]. Previous experiments confirm UCS values remain consistent when the sample dimensions adhere to

this ratio [17-20]; however, a gap exists in the research about the behavior of sample with the same length to diameter ratio and in this paper focus on different behavior of marble, travertine and concrete with the same $\frac{L}{D}$ ratio but different diameter.

Besides the size effect, the shape effect constitutes another crucial parameter for measuring the standard UCS values of rock and concrete. The ASTM recommends using cylindrical and prismatic samples to account for these effects [21]. Du et al. researched the influence of shape on the UCS of white marble samples that were identical in size. According to their findings, cylindrical samples consistently exhibited higher UCS values than their prismatic counterparts [22, 23]. Usually, cubic samples show higher UCS than cylindrical samples, especially for concrete but in rock, because of higher heterogeneity and anisotropy, the result may vary. Experimental studies on various types of rocks have shown that the shape of samples has a significant effect on the UCS values [24-26]. This discovery implies that the shape of samples may be important in determining their mechanical strength properties. Du et al. investigated the effect of geometrical shape on the UCS of white marble samples and found an increase in the UCS with a reduction in the length-to-diameter ratio [22]. Hoek evaluated the rock strength parameters for a constant length-to-diameter ratio and reported that the UCS values of rocks dropped significantly as the sample size rose [27]. Subsequent investigation on prismatic and cylindrical red sandstone samples with a consistent length-to-diameter ratio revealed two trends in compressive strength: UCS values first increased with sample size but then dropped as sample size increased. Simultaneously, UCS was observed to decrease progressively with increasing the sample size, demonstrating the complicated implications of sample dimensions on the compressive strength of rock [28, 29]. Table 1 presents a comprehensive synthesis of findings from previous UCS tests, which cover an assortment of sample sizes and shape configurations. It is noteworthy that the findings of this investigation were compared to those of previous studies to identify differences and similarities.

The influence of sample size and shape on UCS is not the sole factor requiring consideration; these parameters also affect other mechanical properties, such as E and V_p . Larger samples have been found to exhibit increased porosity, which typically leads to a reduction in E. However, research on rock

materials have unveiled a discrepancy in the correlation between sample size and E, accompanied by a notable variability in the E measurements as the sample size increases. Thus, there is no correlation found between higher porosity and lower E values in tuff rock samples, indicating that size and shape have a small effect on E [30]. Studies on particular types of gypsum rock with significant variation in sample size, shape, density, and porosity have revealed that E is generally a function of porosity, with the greatest dispersion of E values occurring at the lowest porosity levels. This dispersion can be ascribed to void clustering. Given the increased number of voids and micro crack that influence the E of a sample, the void clustering becomes less significant at higher porosity levels. The smallest samples have the greatest dispersion, while larger samples have comparable dispersion patterns [31]. According to the authors, no conclusive conclusion was obtained on the tendency of E value variations with increasing the sample size. With increased sample size, reported results for E values indicated fluctuating trends [18, 32, 33]. Inquiries about the length-to-diameter ratio have revealed that a ratio of less than 2 results in a cumulative increase in Elastic Modulus (E) values. When this ratio exceeds 2, a systematic decrease in E values has been observed [32].

Damage mechanics became interested in utilizing wave velocity to examine brittle and quasi-brittle materials such as rocks and concrete because of the special characteristics of non-destructive approaches [34]. Various researchers have investigated the relationships between UCS and V_p , as well as other rock properties [35-41]. However, studies regarding the effect of sample size on V_p are considerably limited. Previous studies show that rocks and concrete pressure wave velocity (V_p) increases with compressive loading but suddenly decreases beyond a certain stress level [42]. Experimental tests on travertine blocks from Iran indicated that increasing the sample diameter reduces the error in measuring V_p . Moreover, V_p values decrease as the sample diameter increases [43].

The exploration of size and shape effects on the mechanical properties of rocks and concrete, including UCS, E and V_p values, has produced statistically nebulous outcomes, underscoring the essential need for more meticulous research. Presently available data fail to establish a decisive statistical correlation, thereby accentuating the intricacy of the size effect [39]. This study scrutinizes how the size and shape of rocks and concrete influence their key mechanical properties, including the toughness at failure, uniaxial compressive strength, elastic modulus, and pressure wave velocity to improve the design of structures that depend on these materials.

Table 1. Summary of previous research on UCS testing with variable sample geometry but same $\frac{L}{D}$

Sample	d (mm)	w (mm)	Shape	L/D	L/w	UCS (MPa)	References
Sandstone	20-150	-	Cylindrical	2	-	79.3-57.5	Kong et al. 2021 [28]
Gosford sandstone	19-145	-	Cylindrical	2	-	34.6-58.8	Masoumi et al. 2016 [44]
Granite	50-110	-	Cylindrical	2	-	125.3-134.3	Thuro et al. 2001 [18]
Limestone	45-80	-	Cylindrical	2	-	186-203.2	
Hollington sandstone	12.5-150	-	Cylindrical	2	-	18.6-34.9	Hawkins 1998 [45]
Pilton sandstone	12.5-150	-	Cylindrical	2	-	136.8-185.5	
Purbeck limestone	12.5-150	-	Cylindrical	2	-	48.8-125.1	
Clifton down limestone	12.5-150	-	Cylindrical	2	-	61.4-140.4	
Bath stone	12.5-150	-	Cylindrical	2	-	9.8-19	
Pennant sandstone	12.5-150	-	Cylindrical	2	-	45.3-92.5	
Burrington oolite limestone	12.5-150	-	Cylindrical	2	-	78-150.6	
Longmont sandstone	25-100	-	Cylindrical	2	-	167.4-172.4	
Kansas limestone	25-150	-	Cylindrical	2	-	48.4-52.3	
Ohya stone	30-400	-	Cylindrical	2	-	6.4-9.9	Yuki et al. 1995 [33]
Lac du bonnet granite	33-294	-	Cylindrical	2	-	168.3-199	Jackson and Lau 1990 [46]
Yellow Limestone	61.5-572.2	-	Cylindrical	2	-	2.1-98.5	Natau et al. 1983 [47]
Ore siderite	22-241	-	Cylindrical	2	-	101-258	Herget and Unruug 1974 [48]
Carthage marble	25-127	-	Cylindrical	2	-	101.2-108.3	Hoskins and Horino 1969 [49]
Salida granite	25-76	-	Cylindrical	2	-	302.3-337.4	
Sanjome andesite	24-70	-	Cylindrical	2	-	97.5-109.6	Nishimatsu et al. 1969 [50]
Ogino tuff	17-70	-	Cylindrical	2	-	56.4-71.3	
Aoishi sandy tuff	13-70	-	Cylindrical	2	-	10.8-43.2	
Shinkomatau andesite	13-70	-	Cylindrical	2	-	209-255	
Inada granite	13-70	-	Cylindrical	2	-	143-192	
Granite	20-60	-	Cylindrical	1	-	17.5-21.9	Lundborg 1967 [51]
Iron ore (in situ test)	-	30-100	Prismatic	-	1	47.5-69.1	Jahns 1966 [52]
Iron ore (laboratory test)	-	5-40	Prismatic	-	1	66.4-112.5	

2. Materials and Methods

2.1. Preparing rock samples

First part of the study examined the influence of rock sample shape and size on the mechanical properties of two distinct types of carbonate rocks: Hersin marble and Haji-Abad travertine. Hersin marble, characterized by dominance of calcite and aragonite minerals, originates from extensive metamorphism and recrystallization of limestone

under significant underground pressure and heat conditions over prolonged periods. Conversely, Haji-Abad travertine, a sedimentary limestone variant, forms through geochemical precipitation at hot water springs, with its porosity attributed to the effervescence of di-carbon dioxide during formation. Cylindrical and prismatic rock samples, as depicted in Figure 1(a), were obtained using industrial sandpaper and a coring device.

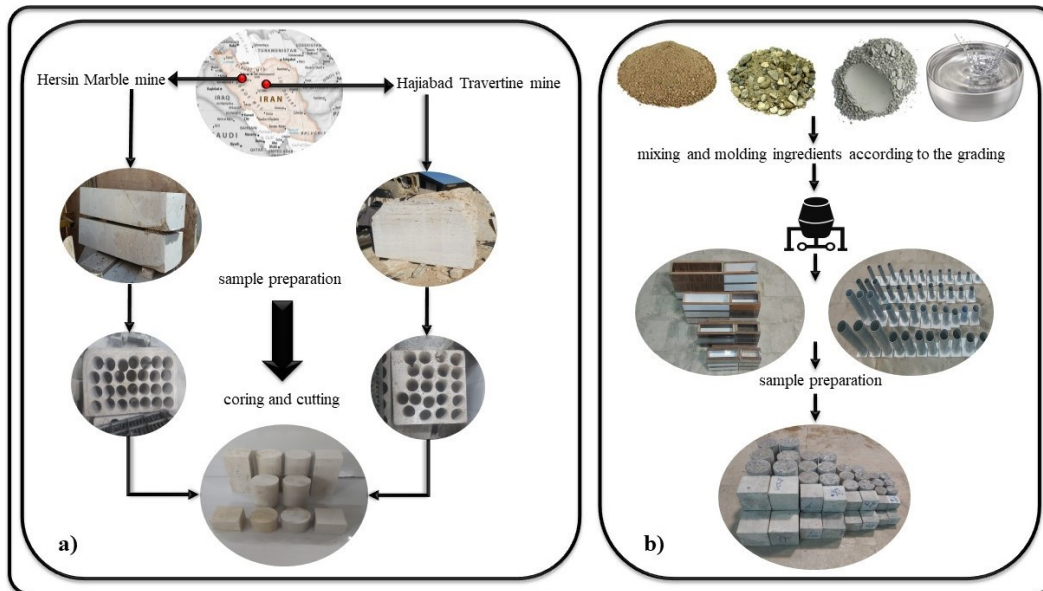


Figure 1. Processing and manufacturing of samples: a) rocks include coring and cutting b) concretes include mixing and curing

2.2. Preparing concrete samples

Second part of this study according to figure 1b, broadens its investigation to explore the impact of size and shape on the mechanical properties of shotcrete concrete. It examines two distinct grain sizes utilized in producing concrete, using Tehran cement type II. Figure 2 illustrates the utilization of concrete with different grain gradations, featuring maximum grain sizes ranging from 0 to 6 mm (concrete 0-6) and 0 to 12 mm (concrete 0-12), in accordance with ASTM C136-01 standards [53]. These concretes were chosen for simultaneous use alongside rock in tunnel construction, fulfilling the role of shotcrete concrete [54]. Table 2 details the design of concrete mixtures, while Table 3 presents comprehensive analytical results for the cement's chemical, physical, and mechanical properties. The mineralogical composition of the cement used in the experiments is depicted in Figure 3. Subsequently, the resulting concrete samples, sharing the same cylindrical and prismatic geometry as the rock samples underwent

mechanical testing following a 28-day curing period. The experimental methods employed are illustrated in Figure 1(b), providing a visual representation of the study's experimental approach.

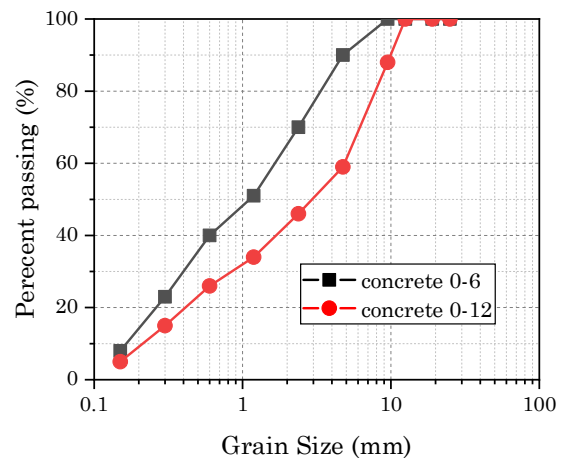


Figure 2. Particle size distribution of two different size of concrete

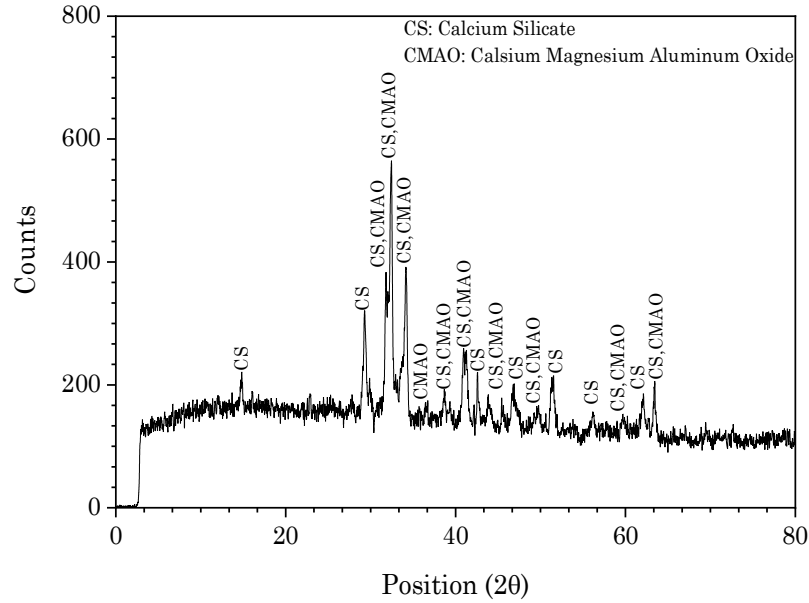


Figure 3. XRD analysis of cement that indicate the main element

Table 2. Concrete mix design

Concrete type	Water (kg/m ³)	Cement (kg/m ³)	Sand (kg/m ³)	Gravel (kg/m ³)
0-12	255.32	441	929.04	632.4
0-6	274.92	480	1311.24	148.76

Table 3. Physical, chemical, and mechanical properties of cement utilized in experiments

Physical, chemical and mechanical properties	Testing Method	Content	Chemical composition	Content (%)
Initial setting time (min)	ASTM C191 – 08 [55]	145	SiO ₂	19.99
Final setting time (min)	ASTM C191 – 08 [55]	210	Al ₂ O ₃	3.09
			Fe ₂ O ₃	2.49
			TiO ₂	0.15
3 days compressive Uniaxial Strength (MPa)	ASTM C109/C109M-20 [56]	23.1	CaO	43.09
7 days compressive Uniaxial Strength (MPa)	ASTM C109/C109M-20 [56]	32.4	MgO	3.88
28 days compressive Uniaxial Strength (MPa)	ASTM C109/C109M-20 [56]	40.8	Na ₂ O	0.25
			K ₂ O	1.04
			P ₂ O ₅	0.07
Specific gravity	ASTM C188 – 95 [57]	3.14	MnO	0.11
Specific surface area (m ² /kg)	ASTM C204 – 07 [57]	324	LOI	19.6

2.3. Arrangement of the sample size and shape

The sample arrangement in Table 4 displays cylindrical samples with length-to-diameter ratios

of 2 and prismatic samples with length-to-side ratios of 1, with both shape sizes being equal to 35, 45, 60, and 75 mm.

Table 4. Arrangement of samples geometry tested in the experiments

Series	Cylindrical			Series	Prismatic			
	d (mm)	L (mm)	L/d		w (mm)	h (mm)	L (mm)	L/(w=h)
UCS-C35	35	70	2	UCS-P35	35	35	35	1
UCS-C45	45	90	2	UCS-P45	45	45	45	1
UCS-C60	60	120	2	UCS-P60	60	60	60	1
UCS-C75	75	150	2	UCS-P75	75	75	75	1

2.4. Relations and review of mechanical specifications

The samples underwent uniaxial compressive strength tests using the ASTM C170/C170M – 09

standard to determine the UCS and E values [21]. The UCS was calculated using Eq. (1), and Eq. (2) was used to calculate E for the linear section of the

stress-strain curve. All tests were carried out at a consistent loading rate of 0.002 mm/s:

$$\sigma = \frac{P_{max}}{A} \quad (1)$$

$$E = \frac{\sigma}{\varepsilon} \quad (2)$$

where σ , P_{max} , A , E and ε are the maximum stress, maximum load, cross-section area, elastic modulus and axial strain, respectively.

The pressure wave velocity V_p was calculated using Eq. (3) according to the ASTM D2845-00 standard [58].

$$V_p = \frac{L}{t} \quad (3)$$

in which V_p , L , and t denote pressure wave velocity, sample length, and the adequate time of propagation and reception of the wave between the gauges of the device, respectively.

2.5. Statistical One-way ANOVA

One-way ANOVA (Analysis of variance) was executed using SPSS software to determine whether there were significant differences in sample sizes within the dataset. The P-value evaluates significance under the null hypothesis assumption, which posits no difference or correlation between sizes. A p-value below 0.05 rejects the null, indicating improbable results by chance. Conversely, a high p-value (greater than

0.05) accepts the null, suggesting chance occurrences. One-way ANOVA evaluates differences in group means based on a single independent variable, checking assumptions such as data independence, normality, and variance homogeneity. Using tests for these ensures data reliability. ANOVA efficiently compares multiple groups to detect significant mean differences, offering more comprehensive insights than simpler tests like t-tests. Its versatility makes it a robust tool for complex statistical analyses in research and experimental studies.

2.6. Loading machine

The experimental tests were conducted at Amirkabir University of Technology using the Dartec-9600 servo-controlled device and the ultrasonic equipment shown in Figures 4 and 5, respectively. The computer-controlled equipment allowed precise control of loading operation and automatic data recording, ensuring reliable results with a uniaxial compressive loading rate of 0.002 mm/s.

3. Experimental results and discussion

Compressive strength tests were performed on cylindrical and prismatic samples. Tables 5 and 6 list the results of the tests on the rocks and concretes, respectively. The results represent the average of the values obtained for three samples tested for each size.

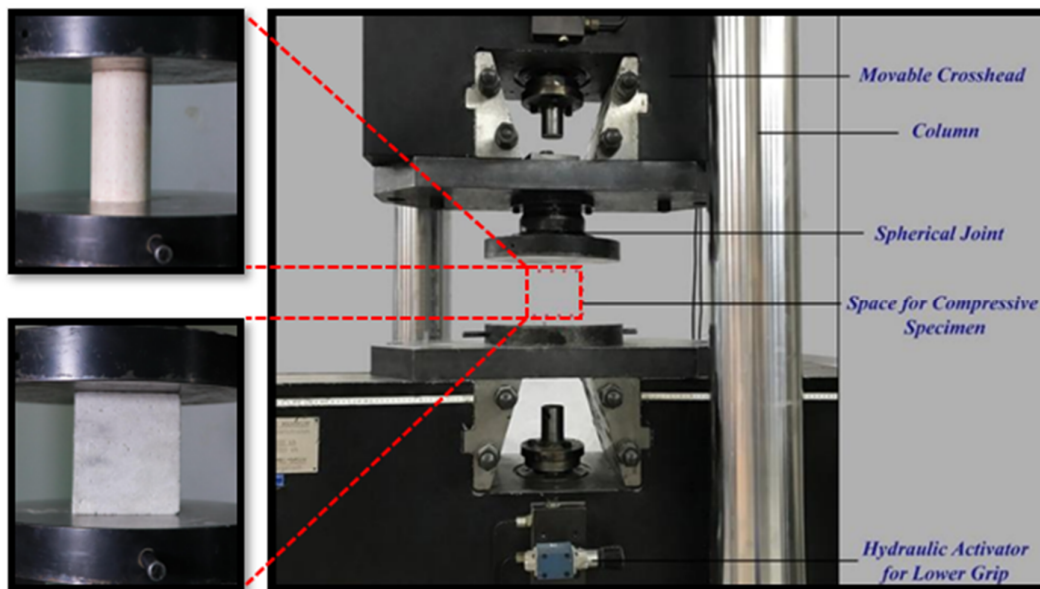


Figure 4. Dartec-9600 servo-controlled device and loading equipment

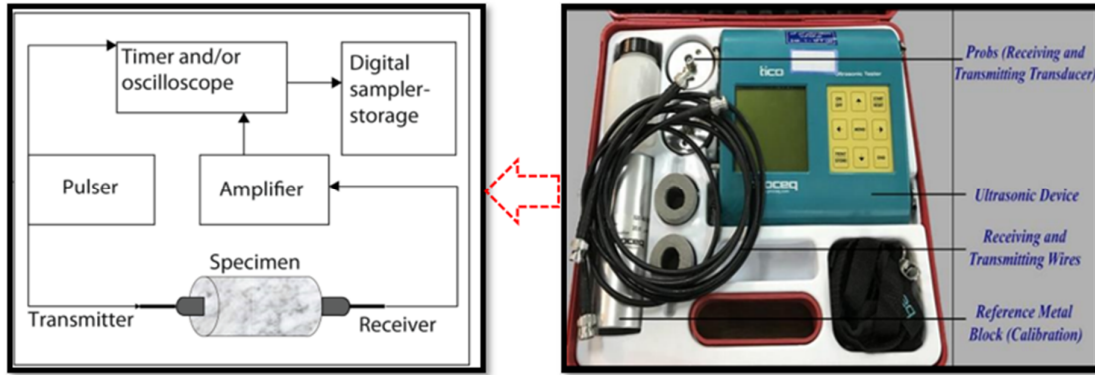


Figure 5. Ultrasonic device and equipment

Table 5. A summary of different information obtained from UCS tests on the rocks

Sample	Marble					Travertine				
	UCS (MPa)	E (GPa)	Vp (m/s)	Toughness (kN.mm)	NS* Post-Peak	UCS (MPa)	E (GPa)	Vp (m/s)	Toughness (kN.mm)	NS* Post-Peak
UCS-C35	74.59	14.26	5836	16.98	-4.00	64.41	11.38	5463	15.52	-4.00
UCS-C45	91.578	16.99	6404	39.10	-4.00	77.00	13.66	5643	34.35	-0.52
UCS-C60	121.51	16.51	6406	149.56	-4.00	96.97	13.59	5540	117.06	-0.30
UCS-C75	101.00	15.30	5880	240.63	-4.00	66.96	13.53	5756	111.86	-3.18
UCS-P35	86.68	5.62	2660	30.19	-0.19	68.93	6.30	2620	23.56	-0.13
UCS-P45	124.71	9.28	3310	95.02	-4.00	102.25	7.33	3360	72.61	-0.13
UCS-P60	136.40	7.86	4480	318.16	-0.52	116.85	6.81	4410	203.87	-0.11
UCS-P75	105.36	7.28	5600	365.17	-0.95	69.29	6.81	5736	153.85	-0.06

*Normalized slope

Table 6. A summary of different information obtained from UCS tests on the concretes

Sample	Concrete 0-6					Concrete 0-12				
	UCS (MPa)	E (GPa)	Vp (m/s)	Toughness (kN.mm)	NS* Post-Peak	UCS (MPa)	E (GPa)	Vp (m/s)	Toughness (kN.mm)	NS* Post-Peak
UCS-C35	52.33	8.39	4116	13.16	-0.39	58.57	7.52	4523	18.41	-0.07
UCS-C45	49.82	9.59	3926	24.37	-0.21	53.37	9.51	4210	27.87	-2.00
UCS-C60	46.20	7.27	4053	65.80	-0.53	45.23	8.64	4340	54.17	-0.29
UCS-C75	39.59	6.50	4113	108.04	-0.17	41.14	6.17	4326	125.81	-0.31
UCS-P35	52.03	4.79	2690	15.41	-0.02	56.70	4.30	2710	24.82	-0.16
UCS-P45	51.46	4.11	3410	34.51	-0.01	52.21	4.74	3380	38.37	-0.17
UCS-P60	46.34	4.16	4053	79.66	-0.02	48.35	4.66	4240	80.70	-0.11
UCS-P75	43.24	3.95	4083	125.27	-0.03	47.52	4.44	4343	141.66	-0.28

*Normalized slope

3.1. Effect of sample geometry on post-peak slopes

Figure 6 depicts the stress-strain curves of rock and concrete samples. The post-peak slopes of cylindrical rocks with different sizes are depicted in Figure 6(c). The stress-strain curves in Figures 6(a) and 6(b) for cylindrical rocks revealed that marble samples did not have post-peak load-carrying capacity, and travertine samples' post-peak slope dropped by 92.50% as sample size increased up to 60 mm, then increased. However, according to the results of cylindrical rock samples, marble samples exhibited greater brittleness. The post-peak slopes of cylindrical concretes with

different sizes are depicted in Figure 6(f). The stress-strain curves in Figures 6(d) and 6(e) for cylindrical concretes indicated that the post-peak slope of concrete samples fluctuated as sample size increased, and concrete 0-12 samples exhibited greater brittleness.

The post-peak slopes of prismatic rocks with different sizes are depicted in Figure 6(i). The stress-strain curves in Figures 6(g) and 6(h) for prismatic rocks revealed that post-peak slopes of marble samples fluctuated as sample size increased. Despite the low variations, the travertine samples' post-peak slope dropped by 53.84% as the sample size increased to 75 mm. However,

according to the results of prismatic rocks, marble samples exhibited greater brittleness. The post-peak slopes of prismatic concretes with different sizes are depicted in Figure 6(l). The stress-strain curves in Figures 6(j) and 6(k) for prismatic concretes indicated that concrete 0-6 samples post-peak slope fluctuated as sample size increased. The post-peak slope for concrete with a maximum grain size of 12 mm dropped by 31.25% as the sample size increased to 60 mm, then increased. On this basis, concrete 0-12 samples exhibited greater brittleness.

The stress-strain curves depicted in Figure 7 show schematically that cylindrical samples, when compared to prismatic ones, possess relatively slender geometries, potentially leading to increased brittleness. Additionally, prismatic samples demonstrate greater flexibility, characterized by a lower post-peak slope, signifying reduced stiffness and higher deformation capacity following peak stress. The results of previous experimental and numerical studies show a strong correlation, confirming the observed similarities in the behavior of the rock and concrete samples [59, 60].

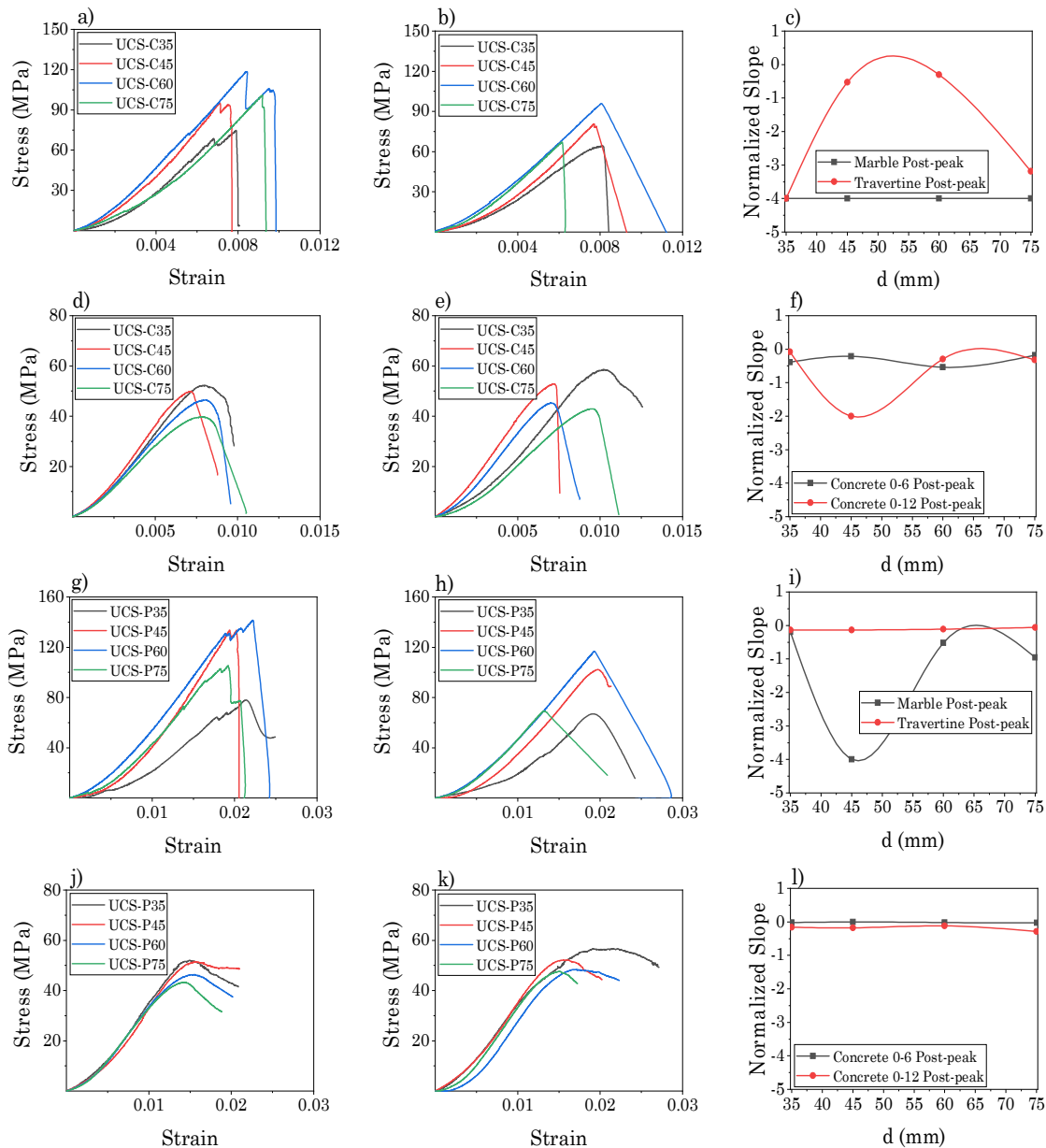


Figure 6. Stress-strain curves and normalized slope: a) cylindrical marble, b) cylindrical travertine, c) cylindrical rocks, d) cylindrical concrete 0-6, e) cylindrical concrete 0-12, f) cylindrical concretes, g) prismatic marble, h) prismatic travertine, i) prismatic rocks, j) prismatic concrete 0-6, k) prismatic concrete 0-12 mm, l) prismatic concretes

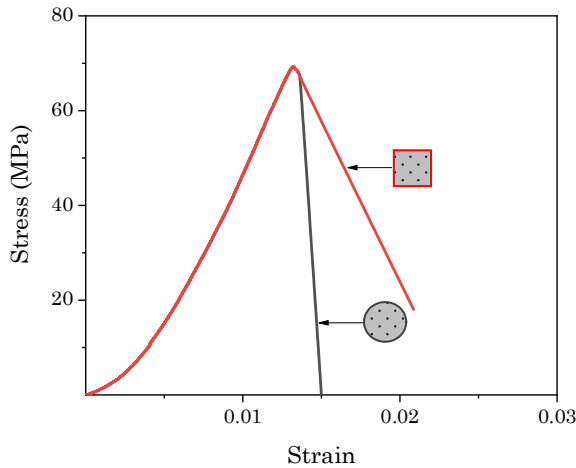


Figure 7. Geometric effects on stress-strain curves after peak.

3.2. Effect of sample geometry on the toughness

Toughness was utilized to assess how sample size, shape, and material type influence the samples' ability to absorb energy before failure. According to the data for the rocks shown in Figure 8(a), the toughness values for cylindrical and

prismatic marble samples increased consistently with the sample size. The toughness of the cylindrical and prismatic travertine samples exhibited a significant increase when the sample size was up to 60 mm. The toughness of the 60-mm cylindrical and prismatic samples was 7.54 and 8.65 times that of the 35-mm ones, respectively. Subsequent to this increase, a decline in toughness was observed. The marble had higher toughness than the travertine. The toughness for cylindrical and prismatic concretes shown in Figure 8(b) increased consistently with the sample size. However, toughness in all sizes of the prismatic concretes had higher values than the cylindrical ones. Furthermore, for cylindrical samples aside from the 60-mm sample, toughness values for concrete 0-12 were higher compared to the concrete 0-6. The toughness values for prismatic concrete 0-12 were also higher than concrete 0-6. The heterogeneity index, porosity, and impurities in travertine samples significantly increased with sample size, leading to a reduction in toughness [28, 60].

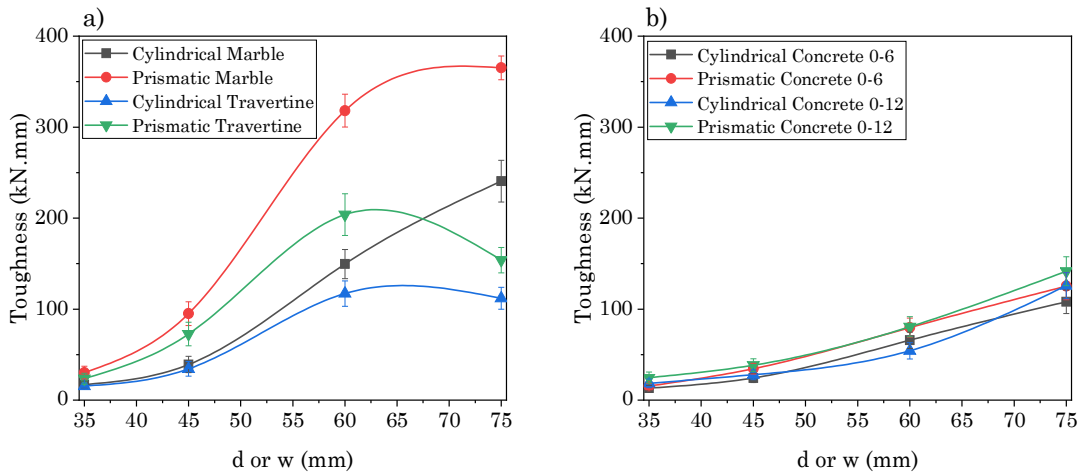


Figure 8. Variations of toughness with increase in sample size: a) rocks b) concretes samples

3.3. Effect of sample geometry on Uniaxial Compressive Strength (UCS)

The UCS values of cylindrical marble and travertine samples shown in Figure 9(a) increased by 62.90% and 50.56%, respectively, with increased sample sizes up to 60 mm and then dropped. A similar trend was observed in the corresponding prismatic samples shown in Figure 9(b) with increases of 57.34% and 69.53%, respectively. Overall, the results indicated higher UCS values of the prismatic rock samples compared to the cylindrical ones. Moreover, for

both sample shapes, marble had higher UCS values than travertine. The observed results are comparable to those of other studies. Increased heterogeneity and porosity in the rock structure brought about by larger sample volumes may result in a lower UCS [28]. However, the sample size should not be smaller or bigger than a particular size to execute the UCS test. This size is specified by the ASTM D2938-95 standard for cylindrical samples with a length-to-diameter ratio of 2-2.5 and a minimum diameter of 54 mm [61]. The UCS data for concretes revealed similar trends for

cylindrical samples in Figure 9(a) and prismatic samples in Figure 9(b). Hence, concretes depicted a decreasing trend in UCS values as sample size increased. However, the cylindrical samples experienced greater reduction than the prismatic ones. The concrete samples showed relatively close UCS values, regardless of size. Nevertheless, the samples with coarser grains experienced a greater drop in UCS, and the UCS values were influenced by factors other than shape and size, such as porosity and heterogeneity, which became more noticeable at greater sample sizes [62]. Moreover, the size and shape of grains, as well as the sample, mortar, or paste, and the concrete transition zone, had a significant role in UCS of concrete samples [63].

Compared to concrete samples, rock samples exhibited more noticeable variations in UCS values with variations in sample size. This discrepancy can be explained by the fact that concrete has significantly lower heterogeneity than rock. However, the concrete composition and structure are uniform due to the materials utilized [27, 60, 64]. Natural rocks exhibit varied mechanical properties affecting their compressive strength and flexibility. Concrete's heterogeneity, from uneven distributions and air bubbles, alters its compressive strength. Porosity in rocks, from voids or local heterogeneities, reduces strength and increases vulnerability. Similarly, porosity in concrete due to air bubbles or uneven distribution diminishes its compressive strength and overall mechanical integrity.

The comparison of the experimental results obtained from this study and previous studies on rock samples reveals two different trends for the UCS as sample size increases:

1. The UCS increases initially as the sample size increases and then drops.
2. The UCS consistently drops as the sample size increases.

The comparison of the results from rock samples with the experimental findings of previous studies, as shown in Figure 10, demonstrates similar results for the rocks used in this study with other rocks such as Kansas Limestone, Longmont Sandstone [49], Iron ore [52], Shinkomatau andesite, Sanjome andesite [50], Clifton Down Limestone, Burrington Oolite Limestone, Pennant Sandstone, Purbeck Limestone, Pilton Sandstone [45], Gosford Sandstone [44], and Sandstone [65]. It is observed that with an increased sample size,

the UCS initially increases and then decreases. Furthermore, previous studies on Salida granite [49], Ore (Siderite) [48], Granite [51], Sandstone [28], Rich ore, Cuprous ore, Cuprous ore, and Impregnated ore [66] demonstrate similar results for concretes. Hence, UCS consistently drops as the sample size increases.

3.4. Effect of sample geometry on Elastic Modulus E

The stress-strain curves from UCS test results were used to estimate elastic modulus E values. The E values for cylindrical and prismatic marble in Figure 11 increased by 19.12% and 65.10%, respectively, with increased sample size up to 45 mm and then dropped. The E values for cylindrical and prismatic travertine samples in Figure 11 increased by 20.07% and 13.36%, respectively, with increased sample size up to 45 mm and then dropped. The E values for cylindrical concretes in Figure 11(a) increased by 14.28% and 26.39%, respectively, with increased sample size up to 45 mm and then dropped. The E values for prismatic concrete 0-12 samples in Figure 11(b) increased by 10.26% as the sample size increased up to 45 mm and then dropped. The E values for prismatic concrete 0-6 samples in Figure 11(b) indicated a fluctuating trend as the sample size increased. The variations for concrete samples followed a pattern consistent with other research findings, and the variation of E values with the increase in the sample size in concrete samples was less than in rocks [18, 62].

Previous studies (Figure 12) exhibited limited findings for the effect of sample size with E values. However, different conclusions emerged as the sample size increased, and most experiments have been reported for samples with diameters smaller or larger than 50 mm. Nevertheless, comparing the results of these studies reveals that, for cylindrical samples, the values of elastic modulus E rose as sample diameter size increased up to 50 mm for Ohya stone [33] and Limestone [18] and then dropped. Similarly, the current experimental results for rocks and concrete samples revealed that E values increased as sample size increased up to 45 mm, then dropped. However, a comparison of the results reveals that porosity in smaller sample sizes is the most influential factor in the dispersion of the E value results [23, 30-32, 60].

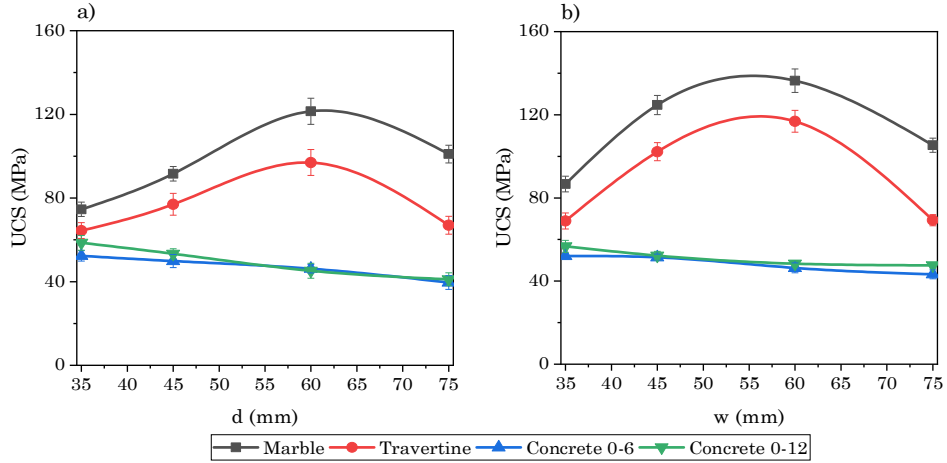


Figure 9. Variations of UCS values as sample size increased: a) cylindrical b) prismatic samples

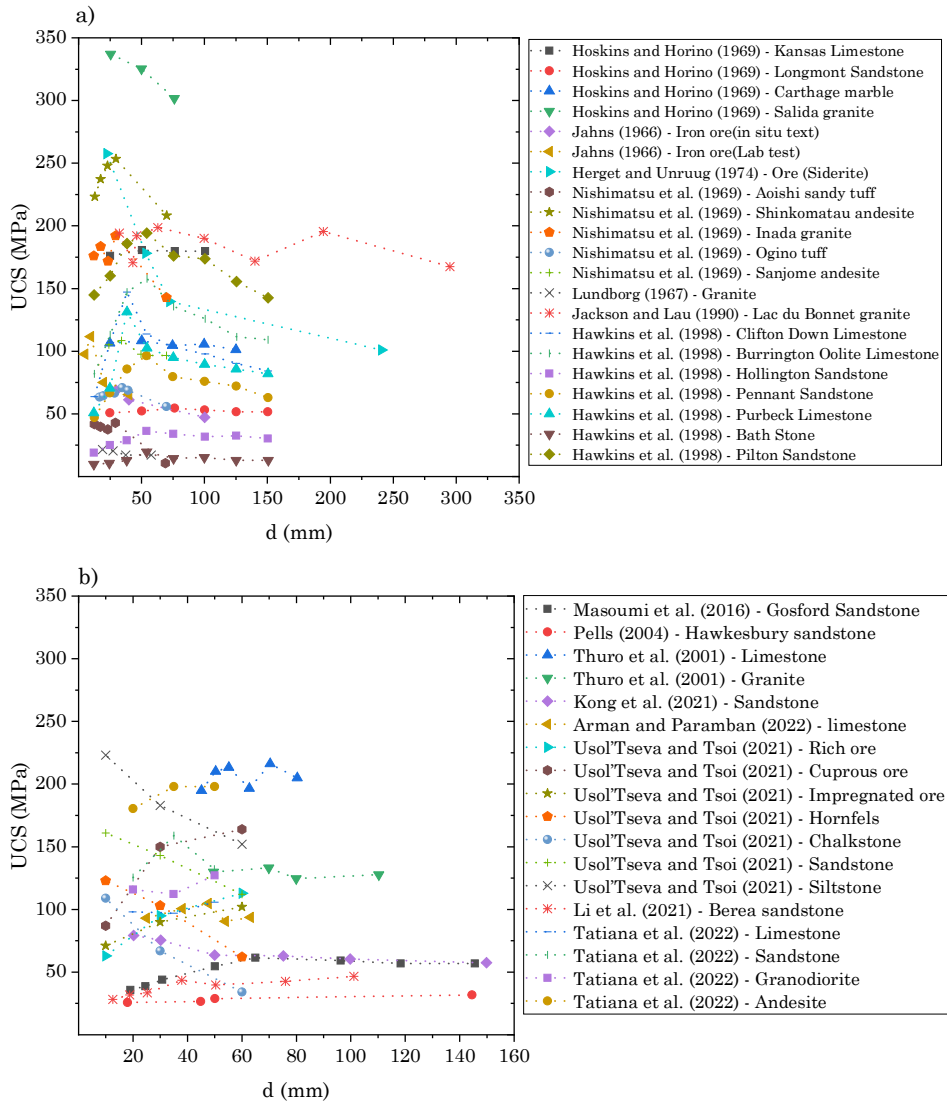


Figure 10. Previous studies on UCS variations as sample size increases: a) before 2000 b) after 2000

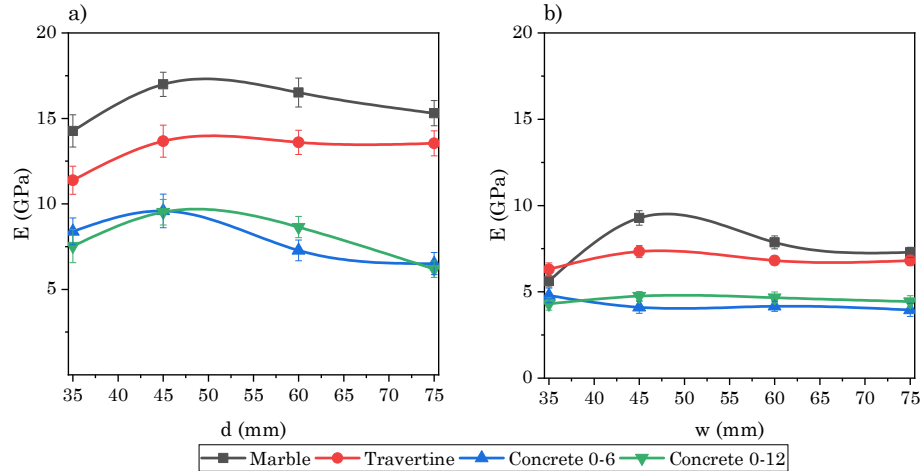


Figure 11. Variations of E values as sample size increases: a) cylindrical b) prismatic samples

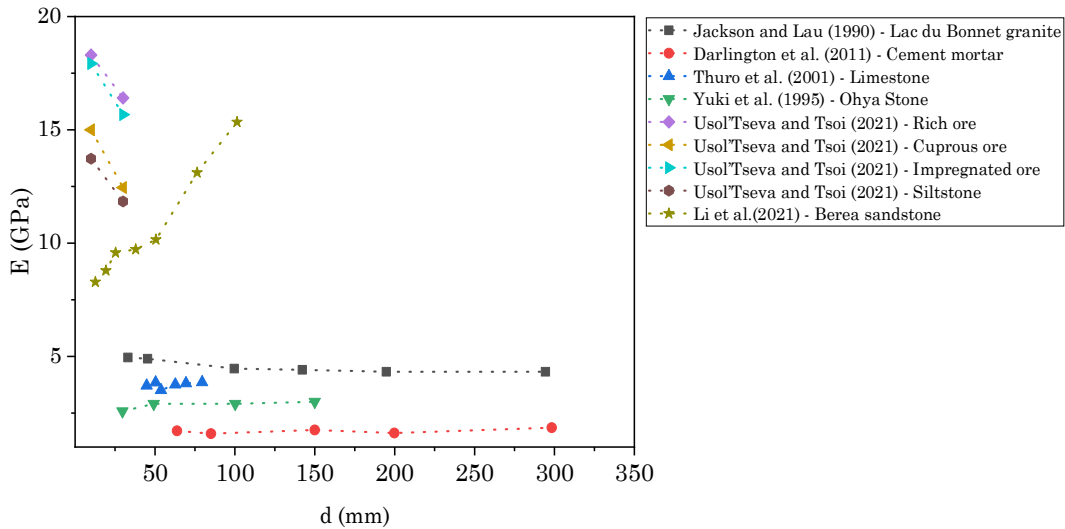


Figure 12. Previous studies on E variations as sample size increases

3.5. The effect of sample geometry on Pressure Wave Velocity (V_p)

Pressure wave velocity (V_p) was computed using Eq. 3 and ultrasonic instrument data. It was found that V_p for cylindrical marble samples shown in Figure 13(a) increased by 9.76% as the sample size increased up to 60 mm and then dropped. However, cylindrical travertine samples shown in Figure 13(a) indicated a fluctuating trend as sample size increased. The V_p values for prismatic rock samples in Figure 13(b) increased with sample size. The V_p values for cylindrical concrete 0-6 samples in Figure 13(a) dropped by 4.61% as the sample size increased up to 45 mm and then increased. Cylindrical concrete 0-12 samples in Figure 13(a) showed a fluctuating trend of V_p values with the increase in the sample size. The V_p

values for prismatic concrete samples in Figure 13(b) consistently increased with the sample size. However, the V_p of prismatic concrete samples tended to reach a constant value as the sample size increased. The fluctuations in V_p of cylindrical samples seem to be due to the increasing volume leading to an increase in heterogeneity, non-uniformity, and porosity [67]. Previous research on V_p of various rock sizes with a length-to-diameter ratio of 2 found that the value of V_p and the inaccuracy in determining it both decrease as sample size increases [43].

Previous studies comparing variations in V_p with increasing sample size are presented in Figure 14. The results demonstrated that most rocks exhibit a variety of trends displaying minor variations in V_p within a limited range. However, within the diameter range of 40 to 60 mm,

significant variations in V_p , including both increases and decreases, have been observed for rocks such as Ignimbrite, Travertine, Granite [67], White and Yellow Atashkoh Travertine, and Red

Dastjerd Onyx Travertine [43]. Similarly, the findings of this study also demonstrate predominantly decreasing or increasing trends in V_p within the diameter range of 45 to 60 mm.

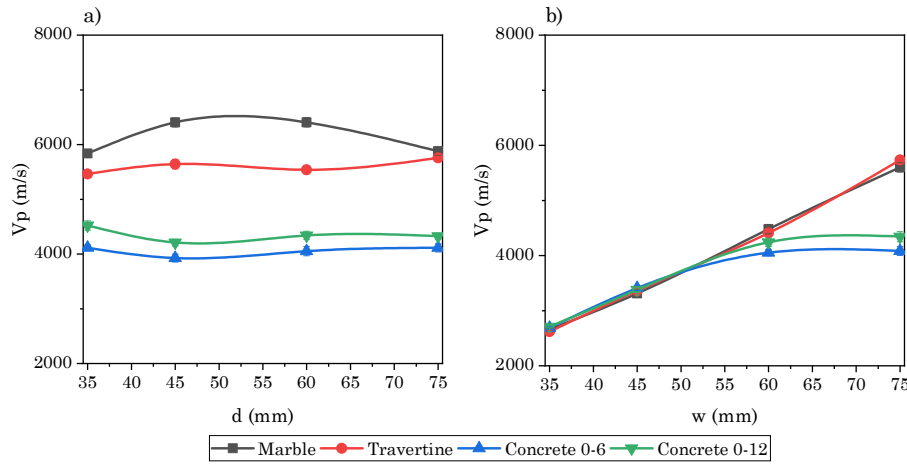


Figure 13. Variations in V_p values with increase in sample size: a) cylindrical, b) prismatic samples

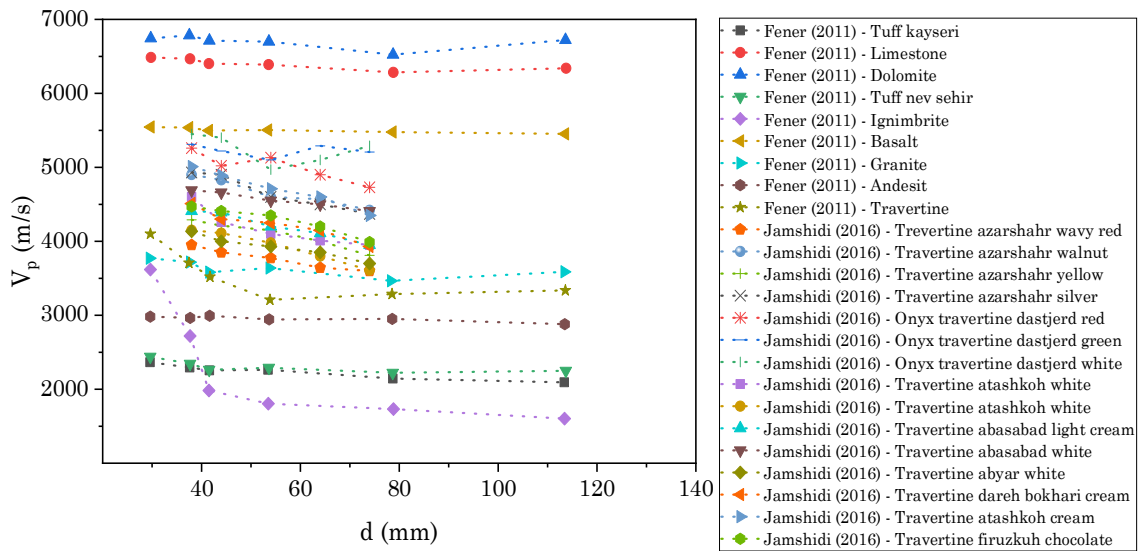


Figure 14. Previous studies on V_p variations with increase in sample size

3.6. Statistical analysis of mechanical characteristics

The statistical analysis results are summarized in Table 7. During a One-way ANOVA, the P-value assesses the likelihood of obtaining results purely by chance. A small P-value (< 0.05) suggests that the observed differences are unlikely to have occurred randomly, leading to rejection of the null hypothesis. Conversely, a large P-value (> 0.05) indicates that the observed differences could plausibly happen by chance alone, thus failing to reject the null hypothesis. Statistical analysis revealed significant variations in UCS for rocks.

However, for concrete 0-12 samples and cylindrical concrete 0-6 samples, no significant variations were observed. This result is likely attributable to the selection of materials in the concrete mix design, leading to a favorable density and uniformity in the sample structure [63, 64]. Consequently, in the case of concrete samples with appropriate homogeneity and uniformity, the effect of size and shape on UCS results was minimal. In contrast, due to the non-uniform and heterogeneous structure of the rock samples, the sample size and shape had a significant effect on UCS [27, 64]. The statistical analysis results of variations in E for both rocks and concretes, except for prismatic marble

samples, did not demonstrate satisfactory levels of statistical significance. Consequently, it can be inferred that, for both rocks and concrete, the sample size and shape exerted minimal influence on the E values. This is presumably the reason why no clear and consistent pattern has been found in the variations of E values in previous studies [18, 32, 33, 46, 64, 66, 68]. Statistical analysis results for variations in V_p for cylindrical travertine and concrete samples did not exhibit significant and

desirable variations. The porous structure of travertine may manifest as clustering of cavities in larger-size samples, affecting V_p variations. Furthermore, in cylindrical concrete samples, due to their homogeneous and uniform structure [60, 67], the size of the sample had no significant effect on the values of V_p . Drawing insights from the statistical analysis, it is evident that the size and shape of the samples significantly influence UCS and V_p values of rocks.

Table 7. Summary of ANOVA results for UCS, E, and V_p

Dependent Variable	(I) size	(J) size	MD ¹ (UCS)	MD (E)	MD (V_p)	SE ² (UCS)	SE (E)	SE (V_p)	p-value ³ (UCS)	p-value (E)	p-value (V_p)
Marble (Prismatic)	35	45	-38.02	-3.66	-650	3.64	0.29	56.38	0.000	0.000	0.000
		60	-49.71	-2.24	-1820	3.64	0.29	56.38	0.000	0.000	0.000
		75	-18.67	-1.66	-2940	3.64	0.29	56.38	0.004	0.002	0.000
	45	60	-11.68	1.42	-1170	3.64	0.29	56.38	0.050	0.006	0.000
		75	19.34	2	-2290	3.64	0.29	56.38	0.003	0.001	0.000
		60	75	31.03	0.58	-1120	3.64	0.29	56.38	0.000	0.270
Marble (Cylindrical)	35	45	-16.98	-2.73	-570	3.66	0.66	63.30	0.007	0.015	0.000
		60	-46.92	-2.25	-572	3.66	0.66	63.30	0.000	0.039	0.000
		75	-26.41	-1.04	-46	3.66	0.66	63.30	0.000	0.448	0.884
	45	60	-29.93	0.48	-2.00	3.66	0.66	63.30	0.000	0.886	1.000
		75	-9.43	1.69	524	3.66	0.66	63.30	0.122	0.127	0.000
		60	75	20.50	1.21	526	3.66	0.66	63.30	0.002	0.332
Travertine (Prismatic)	35	45	-33.32	-1.04	-740	3.37	0.26	47.69	0.000	0.018	0.000
		60	-47.92	-0.52	-1790	3.37	0.26	47.69	0.000	0.276	0.000
		75	-0.36	-0.52	-3116	3.37	0.26	47.69	1.000	0.276	0.000
	45	60	-14.59	0.52	-1050	3.37	0.26	47.69	0.011	0.276	0.000
		75	32.95	0.52	-2376	3.37	0.26	47.69	0.000	0.276	0.000
		60	75	47.55	0	-1326	3.37	0.26	47.69	0.000	1.000
Travertine (Cylindrical)	35	45	-12.59	-2.28	-180	4.05	0.65	57.66	0.057	0.034	0.056
		60	-32.56	-2.21	-77	4.05	0.65	57.66	0.000	0.040	0.568
		75	-2.55	-2.15	-293	4.05	0.65	57.66	0.919	0.045	0.004
	45	60	-19.97	0.07	103	4.05	0.65	57.66	0.005	1.000	0.345
		75	10.04	0.13	-113	4.05	0.65	57.66	0.139	0.997	0.278
		60	75	30.01	0.06	-216	4.05	0.65	57.66	0.000	1.000
Concrete 0-6 (Prismatic)	35	45	0.57	0.68	-720	1.51	0.29	45.36	0.981	0.179	0.000
		60	5.68	0.63	-1363	1.51	0.29	45.36	0.023	0.224	0.000
		75	8.78	0.84	-1393	1.51	0.29	45.36	0.002	0.084	0.000
	45	60	5.11	-0.05	-643	1.51	0.29	45.36	0.039	0.998	0.000
		75	8.21	0.16	-673	1.51	0.29	45.36	0.003	0.947	0.000
		60	75	3.09	0.21	-30	1.51	0.29	45.36	0.250	0.891
Concrete 0-6 (Cylindrical)	35	45	2.50	-1.20	172	2.26	0.62	55.94	0.695	0.296	0.060
		60	6.13	1.12	45	2.26	0.62	55.94	0.101	0.346	0.851
		75	12.74	1.89	-15	2.26	0.62	55.94	0.002	0.065	0.993
	45	60	3.62	2.32	-127	2.26	0.62	55.94	0.430	0.025	0.184
		75	10.23	3.09	-187	2.26	0.62	55.94	0.008	0.005	0.041
		60	75	6.61	0.77	-60.00	2.26	0.62	55.94	0.075	0.629
Concrete 0-12 (Prismatic)	35	45	4.49	-0.44	-676	1.65	0.26	50.63	0.099	0.402	0.000
		60	8.34	-0.36	-1530	1.65	0.26	50.63	0.004	0.556	0.000
		75	9.17	-0.14	-1633	1.65	0.26	50.63	0.002	0.950	0.000
	45	60	3.85	0.08	-853	1.65	0.26	50.63	0.169	0.990	0.000
		75	4.68	0.30	-956	1.65	0.26	50.63	0.084	0.682	0.000
		60	75	0.83	0.22	-103	1.65	0.26	50.63	0.956	0.839
Concrete 0-12 (Cylindrical)	35	45	5.20	-1.99	313	2.59	0.59	56.97	0.263	0.041	0.003
		60	13.34	-1.12	183	2.59	0.59	56.97	0.004	0.306	0.049
		75	17.43	1.35	197	2.59	0.59	56.97	0.001	0.184	0.035
	45	60	8.13	0.87	-130	2.59	0.59	56.97	0.055	0.499	0.182
		75	12.22	3.34	-116	2.59	0.59	56.97	0.007	0.002	0.252
		60	75	4.08	2.47	14	2.59	0.59	56.97	0.443	0.014

¹ MD: Mean difference is a subtraction of J group mean from I

² SE: Standard error of the mean for each size being compared

³ p-value is significant at the 0.05 level

4. Conclusions

This study explores the impact of the size and shape of rocks and concrete on their mechanical properties, such as Toughness at Failure, Uniaxial Compressive Strength (UCS), Elastic Modulus (E), and Pressure Wave Velocity (V_p). Understanding these influences is crucial for improving the design and performance of structures that utilize these materials. The investigation is divided into three main sections: Size Effect, which looks at how varying dimensions affect properties; Shape Effect, which examines the role of different geometries; and Material Type Effect, which considers how different compositions of rocks and concrete respond under mechanical characteristics. The insights gained aim to inform better structural design practices.

Size Effect

- To study the size effect, the UCS values for cylindrical and prismatic rock samples increased with the sample size and then dropped, indicating that the dimensions of the rock samples cannot be lower or higher than a specific size.
- The UCS values for cylindrical and prismatic concrete samples dropped as the sample size increased. Furthermore, the UCS values for concrete samples with coarser aggregate experienced more reduction than finer-grained ones.
- The UCS values of prismatic rock and concrete samples were higher than those of cylindrical samples with equivalent dimensions.
- The E values for cylindrical and prismatic rock samples and cylindrical concrete samples increased with the sample size and then dropped. However, the variations of E values for prismatic concrete samples were minor.
- The V_p values of prismatic rock and concrete samples increased as the size of the samples increased, whereas prismatic concretes exhibited a tendency to reach a constant value as sample size increased. In contrast, cylindrical samples exhibited varied trends with increasing sample size, such that both heterogeneity and porosity increased as size increased, thereby impacting V_p values. This emphasizes the influence of sample geometry on V_p behavior in both rock and concrete.

Shape Effect

- To study the shape effect on UCS, the stress-strain curves of the prismatic rock and concrete

samples in figures 6 and 7, revealed greater post-peak flexibility and ductility than cylindrical samples. The prismatic samples indicated a greater ability to absorb load and resist the variety in the sample shape. They appear to be a reliable representative for testing brittle and quasi-brittle materials.

- The statistical analysis revealed that the sample geometry had a significant effect on UCS and V_p values of the rocks.

Effect of Type of material

- The constituent materials of the concrete samples were selected, rendering them more homogeneous compared to rocks. Consequently, as the sample volume increased, the fluctuations in UCS values for concrete were lower than those for rocks.

References

- [1]. Li, M., Hao, H., Shi, Y., & Hao, Y. (2018). Specimen shape and size effects on the concrete compressive strength under static and dynamic tests. *Construction and Building Materials*, 161, 84-93.
- [2]. Feng, F., Li, X., Rostami, J., Peng, D., Li, D., & Du, K. (2019). Numerical investigation of hard rock strength and fracturing under polyaxial compression based on Mogi-Coulomb failure criterion. *International Journal of Geomechanics*, 19(4).
- [3]. Mohammadifar, M., Asheghi M.T., & Fahimifar, A. (2024). Parametric and Sensitivity Analysis on the Effects of Geotechnical Parameters on Tunnel Lining in Soil Surrounding. *Journal of Structural and Construction Engineering (JSCE)*.
- [4]. Kazempour, O., Moosazadeh, S., Qarahasanlou, A.N., & Baghban G.M.R. (2024). Urban Tunneling Risk Management: Ground Settlement Assessment through Proportional Hazards Modeling. *Journal of Mining and Environment*, 15(3), 1161-1175.
- [5]. Khalili, S., Monjezi, M., Amini, K.H., & Saghat forosh, A. (2024). Evaluation the Effect of Blast Pattern on Post-Failure Rate around the Miyaneh-Ardabil Railway Tunnel. *Journal of Mining and Environment*, 15(3), 1149-1160.
- [6]. Mohammadifar, M., Asheghi Mehmamandari, T., & Mirjafari, SA. (2024). Discovering the optimal distance between spatial orthogonal tunnels: A dynamic analysis using Tehran metro as a case study. *Insight - Civil Engineering*. 2024; 7(1): 613.
- [7]. Mogi, K. (1966). Some precise measurements of fracture strength of rocks under uniform compressive stress. *Felsmech, Ingenieurgeol*, 4(1), 41.
- [8]. Obert, L., & Duvall, W.I. (1967). Rock mechanics and the design of structures in rock. *John Wiley & Sons, Inc.*

- [9]. John, M. (1972). The Influence of Length to Diameter Ratio on Rock Properties in Uniaxial Compression, A Contribution to Standardization in Rock Mechanics Testing; Report South African CSIR No ME1083/5, Council for Scientific and Industrial Research, Pretoria, South Africa. *Int J Rock Mech Min Sci*, 438, 12771287.
- [10]. Labuz, J.F., & Bridell, J. (1993). Reducing frictional constraint in compression testing through lubrication. *International journal of rock mechanics and mining sciences & geomechanics abstracts*, 30(4), 451-455.
- [11]. Mogi, K. (2006). Experimental rock mechanics. *The Netherlands, Taylor and Francis Balkema*.
- [12]. Pan, P.Z., Feng, X.T., & Hudson, J.A. (2009). Study of failure and scale effects in rocks under uniaxial compression using 3D cellular automata. *International Journal of Rock Mechanics and Mining Sciences*, 46(4), 674-685.
- [13]. Omid Manesh, M., Sarfarazi, V., Babanouri, N., & Rezaei, A. (2023) Investigation of External Work, Fracture Energy, and Fracture Toughness of Oil Well Cement Sheath using HCCD Test and CSTBD Test. *Journal of Mining and Environment*, 14(2), 619-634.
- [14]. Omid Manesh, M., Sarfarazi, V., Babanouri, N., & Rezaei, A. (2023) Investigation of Fracture Toughness of Shotcrete using Semi-Circular Bend Test and Notched Brazilian Disc test; Experimental Test and Numerical Approach. *Journal of Mining and Environment*, 14(1), 233-242.
- [15]. Yavari, M.D., Haeri, H., Sarfarazi, V., Fatehi Marji, M., & Lazemi H.A. (2021) On Propagation Mechanism of Cracks Emanating from Two Neighboring Holes in Cubic Concrete Specimens under Various Lateral Confinements. *Journal of Mining and Environment*, 12(4), 1003-1017.
- [16]. ASTM, D7012-14. (2004). Standard Test Methods for Compressive Strength and Elastic Moduli of Intact Rock Core Specimens under Varying States of Stress and Temperatures. *ASTM, West Conshohocken, PA, USA*.
- [17]. Hudson, J.A., Crouch, S.L., & Fairhurst, C. (1972). Crouch, and C. Fairhurst, Soft, stiff and servo-controlled testing machines: a review with reference to rock failure. *Engineering Geology*, 6(3), 155-189.
- [18]. Thuro, K., Plinninger, R., Zäh, S., & Schütz, S. (2001). Scale effects in rock strength properties, Part 1: Unconfined compressive test and Brazilian test. *ISRM regional symposium, EUROCK*.
- [19]. Tuncay, E., & Hasancebi, N. (2009). The effect of length to diameter ratio of test specimens on the uniaxial compressive strength of rock. *Bulletin of engineering geology and the environment*, 68, 491-497.
- [20]. Liang, C., Zhang, Q., Li, X., & Xin, P. (2016). The effect of specimen shape and strain rate on uniaxial compressive behavior of rock material. *Bulletin of Engineering Geology and the Environment*, 75, 1669-1681.
- [21]. ASTM, C170/C170M-09. (2009). Standard Test Method for Compressive Strength of Dimension Stone. *ASTM, West Conshohocken, PA, USA*.
- [22]. Du, K., Su, R., Tao, M., Yang, C., Momeni, A., & Wang, S. (2019). Specimen shape and cross-section effects on the mechanical properties of rocks under uniaxial compressive stress. *Bulletin of Engineering Geology and the Environment*, 78, 6061-6074.
- [23]. Nasari, A., Ghasemi, O., Asghari, A., Fahimifar, A., & Havaei, G. (2023). Influence of Geometry (Size and Shape) on the Correlation Between Strength Properties and Point Load Strength Index of Brittle Materials. *13th International Congress on Civil Engineering, University of Science and Technology, Tehran, Iran*.
- [24]. Li, D., Li, C.C., & Li, X. (2011). Influence of sample height-to-width ratios on failure mode for rectangular prism samples of hard rock loaded in uniaxial compression. *Rock Mechanics and Rock Engineering*, 44, 253-267.
- [25]. Asheghi Mehmandari, T., Mohammadi, D., Ahmadi, M. & Mohammadifar, M. (2024) Fracture mechanism and ductility performances of fiber reinforced shotcrete under flexural loading insights from digital image correlation (DIC). *Insight - Civil Engineering*. 2024; 7(1): 611.
- [26]. Du, K., Tao, M., Li, X., & Zhou, J. (2016). Experimental study of slabbing and rockburst induced by true-triaxial unloading and local dynamic disturbance. *Rock Mechanics and Rock Engineering*, 49, 3437-3453.
- [27]. Hoek, E. (2000). Practical rock engineering, Course notes by Evert Hoek. *AA Balkema Publishers, Rotterdam, Netherlands*.
- [28]. Kong, X., Liu, Q., & Lu, H. (2021). Effects of rock specimen size on mechanical properties in laboratory testing. *Journal of Geotechnical and Geoenvironmental Engineering*, 147(5), 04021013.
- [29]. Asheghi Mehmandari, T. & Alizadeh, H. (2023). Engineering Concept and Construction Methods of High-Rise Building. *Sanei Publisher, Tehran, 308 P*.
- [30]. Hudyma, N., Avar, B.B., & Karakouzian, M. (2004). Compressive strength and failure modes of lithophysae-rich Topopah Spring Tuff specimens and analog models containing cavities. *Engineering Geology*, 73(1-2), 179-190.
- [31]. Puppala, A.J., Hudyma, N., & Likos, W.J. (2007). Problematic Soils and Rocks and In Situ Characterization. *American Society of Civil Engineers*.

- [32]. Meng, Q., Zhang, M., Han, L., Pu, H., & Li, H. (2016). Effects of size and strain rate on the mechanical behaviors of rock specimens under uniaxial compression. *Arabian Journal of Geosciences*, 9, 1-14.
- [33]. Yuki, N., Aoto, S., Ogata, Y., & Yoshinaka, R. (1995). The scale and creep effects on strength of welded tuff. *Rock foundation*, 219-222.
- [34]. Zare, P., Asheghi, M.T., Fahimifar, A., & Zabetian, S. (2020). Experimental Assessment of Damage and Crack Propagation Mechanism in Heterogeneous Rocks. *5th International Conference on Applied Research in Science and Engineering, University of Amsterdam, Netherlands*.
- [35]. Kahraman, S. (2001). Evaluation of simple methods for assessing the uniaxial compressive strength of rock. *International Journal of Rock Mechanics and Mining Sciences*, 38(7), 981-994.
- [36]. Yasar, E., & Erdogan, Y. (2004). Correlating sound velocity with the density, compressive strength and Young's modulus of carbonate rocks. *International Journal of Rock Mechanics and Mining Sciences*, 41(5), 871-875.
- [37]. Sharma, P., & Singh, T. (2008). correlation between P-wave velocity, impact strength index, slake durability index and uniaxial compressive strength. *Bulletin of Engineering Geology and the Environment*, 67, 17-22.
- [38]. Yagiz, S. (2009). Predicting uniaxial compressive strength, modulus of elasticity and index properties of rocks using the Schmidt hammer. *Bulletin of engineering geology and the environment*, 68, 55-63.
- [39]. Diamantis, K., Bellas, S., Migiros, G., & Gartzos, E. (2011). Correlating wave velocities with physical, mechanical properties and petrographic characteristics of peridotites from the central Greece. *Geotechnical and Geological Engineering*, 29, 1049-1062.
- [40]. Yagiz, S. (2011). P-wave velocity test for assessment of geotechnical properties of some rock materials. *Bulletin of Materials Science*, 34, 947-953.
- [41]. Sarkar, K., Vishal, V., & Singh, T. (2012). An empirical correlation of index geomechanical parameters with the compressional wave velocity. *Geotechnical and Geological Engineering*, 30, 469-479.
- [42]. Asheghi, M.T., Fahimifar, A., & Asemi, F. (2020). The Effect of the Crack Initiation and Propagation on the P-Wave Velocity of Limestone and Plaster Subjected to Compressive Loading. *AUT Journal of Civil Engineering*, 4(1), 55-62.
- [43]. Jamshidi, A., Nikudel, M.R., Khomehchiyan, M., & Sahamieh, R.Z. (2016). The effect of specimen diameter size on uniaxial compressive strength, P-wave velocity and the correlation between them. *Geomechanics and Geoengineering*, 11(1), 13-19.
- [44]. Masoumi, H., Saydam, S., & Hagan, P.C. (2016). Unified size-effect law for intact rock. *International Journal of Geomechanics*, 16(2), 04015059.
- [45]. Hawkins, A. (1998). Aspects of rock strength. *Bulletin of Engineering Geology and the Environment*, 57, 17-30.
- [46]. Jackson, R., & Lau, J. (1990). The effect of specimen size on the laboratory mechanical properties of Lac du Bonnet grey granite. *International workshop on scale effects in rock masses*.
- [47]. Natau, O.P., Frohlich, B.O., & Mutschler, T.O. (1983). Recent developments of the large scale triaxial test. *5th ISRM Congress*.
- [48]. Herget, G., & Unrug, K. (1974). In-situ strength prediction of mine pillars based on laboratory tests. *3rd Congress of the Int. Society for Rock Mechanics*.
- [49]. Hoskins, J.R., & Horino, F.G. (1969). Influence of Spherical Head Size and Specimen Diameters on the Uniaxial Compressive Strength of Rocks. *Department of the Interior, Bureau of Mines, United State*.
- [50]. Nishimatsu, Y., Yamaguchi, U., Motosugi, K., & Morita, M. (1969). The size effect and experimental error of the strength of rocks. *J Min Mat Proc Inst Jpn*, 18, 1019-1025.
- [51]. Lundborg, N. (1967). The strength-size relation of granite. *International Journal of Rock Mechanics and Mining Sciences & Geomechanics Abstracts*, 4(3), 269-272.
- [52]. Jahns, H. (1966). Measuring the strength of rock in situ at an increasing scale. *ISRM Congress*.
- [53]. ASTM, C136-01. (2001). Standard Test Method for Sieve Analysis of Fine and Coarse Aggregates. *ASTM, West Conshohocken, PA, USA*.
- [54]. Mehmandari, T.A., Shokouhian, M., Imani, M., & Fahimifar, A. (2024). Experimental and numerical analysis of tunnel primary support using recycled, and hybrid fiber reinforced shotcrete. *Structures, Elsevier*, 63, 106282.
- [55]. ASTM, C191-08. (2008). Standard Test Methods for Time of Setting of Hydraulic Cement by Vicat Needle. *ASTM, West Conshohocken, PA, USA*.
- [56]. ASTM, C109/C109M-20. (2008). Standard Test Method for Compressive Strength of Hydraulic Cement Mortars (Using 2-in. or [50-mm] Cube Specimens). *ASTM, West Conshohocken, PA, USA*.
- [57]. ASTM, C188-95. (2003). Standard Test Method for Density of Hydraulic Cement. *ASTM, West Conshohocken, PA, USA*.
- [58]. ASTM, D2845-00. (2000). Standard Test Method for Laboratory Determination of Pulse

Velocities and Ultrasonic Elastic Constants of Rock. *ASTM, West Conshohocken, PA, USA*.

[59]. Xu, Y., & Cai, M. (2017). Numerical study on the influence of cross-sectional shape on strength and deformation behaviors of rocks under uniaxial compression. *Computers and Geotechnics*, 84, 129-137.

[60]. Naseri, A., Fattahi, S.M., Shokri, F., Hosseinnia, A., & Fahimifar, A. (2024). Exploring the Influence of Sample Geometry on the Tensile Strength of Rock and Concrete: An Integrated Experimental and Numerical Analysis. *Iranian Journal of Science and Technology, Transactions of Civil Engineering*.

[61]. ASTM, D2938-95. (2002). Standard test method for unconfined compressive strength of intact rock core specimens. *ASTM, West Conshohocken, PA, USA*.

[62]. Zhang, C., Lin, H., Qiu, C., Jiang, T., & Zhang, J. (2020). The effect of cross-section shape on deformation, damage and failure of rock-like materials under uniaxial compression from both a macro and micro viewpoint. *International Journal of Damage Mechanics*, 29(7), 1076-1099.

[63]. Mehta, P.K., & Monteiro, P. (2006). Concrete: microstructure, properties, and materials. *McGraw Hill*.

[64]. Darlington, W.J., Ranjith, P.G., & Choi, S. (2011). The effect of specimen size on strength and other properties in laboratory testing of rock and rock-like cementitious brittle materials. *Rock mechanics and rock engineering*, 44, 513-529.

[65]. Tatiana, D., Martin, B., Petra, D., & Renáta, A. (2022). Influence of specimen size and shape on the uniaxial compressive strength values of selected Western Carpathians rocks. *Environmental Earth Sciences*, 81(9).

[66]. Usoltseva, O.M., & Tsoi, P.A. (2021). The Influence of Size Effect on Strength and Deformation Characteristics of Different Types of Rock Samples. *International science and technology conference Earth science, Vladivostok, Russian Federation*.

[67]. Fener, M. (2011). The effect of rock sample dimension on the P-wave velocity. *Journal of Nondestructive Evaluation*, 30, 99-105.

[68]. Li, H., Song, K., Tang, M., Qin, M., Liu, Z., Qu, M., Li, B., & Li, Y. (2021). Determination of scale effects on mechanical properties of Berea Sandstone. *Geofluids*, 1-12.

بررسی تأثیر تغییرات هندسی نمونه‌های سنگ و بتن بر روی خصوصیات مکانیکی آن‌ها

امیرحسین ناصری^۱، بهنام ملکی^۲، توحید عاشقی مهمانداری^۲، امین توحیدی^۲ و احمد فهیمی فر^{۲*}

۱- دانشکده گرمساره، دانشگاه صنعتی امیرکبیر، تهران، ایران

۲- دانشکده عمران و محیط زیست، دانشگاه صنعتی امیرکبیر، تهران، ایران

۳- دانشکده مهندسی معدن، دانشگاه صنعتی امیرکبیر، تهران، ایران

ارسال ۲۰۲۴/۰۶/۰۴، پذیرش ۲۰۲۴/۰۸/۰۴

* نویسنده مسئول مکاتبات: fahim@aut.ac.ir

چکیده:

مطالعه حاضر به بررسی تأثیر اندازه نمونه و هندسه بر رفتار مکانیکی سنگ و بتن می‌پردازد. به طور خاص، عواملی از جمله مقاومت فشاری تک محوری (UCS)، مدول الاستیک (E) و سرعت موج فشار (V_p) را بررسی می‌کند. نتایج بررسی‌های فوق‌الذکر نشان داد که همبستگی قابل توجهی بین ابعاد و مورفولوژی نمونه‌ها با این ویژگی‌ها وجود دارد. همه آزمایش‌ها با نرخ بارگذاری یکنواخت ۰.۰۰۲ میلی‌متر بر ثانیه انجام شد. با توجه به نتایج، اثر اندازه و شکل نمونه بر UCS برای بتن بیشتر از سنگ قابل پیش بینی است. افزایش حجم نمونه منجر به افزایش اولیه و به دنبال آن کاهش در مقادیر UCS سنگ‌ها شد. علاوه بر این، بتن به طور معمول با افزایش اندازه نمونه، کاهش در مقادیر UCS نشان داد. مقادیر UCS و E ابتدا قبل از سقوط افزایش یافتند که نشان دهنده وجود تأثیر حجم نمونه بر حداکثر UCS است. مقادیر V_p نمونه‌های سنگ و بتن منشوری به طور مداوم افزایش یافت. پس از دستیابی به مقاومت بهینه، نمونه‌های منشوری به دلیل رفتار پس از اوج، درجات انعطاف‌پذیری و شکل‌پذیری بیشتری را نسبت به نمونه‌های استوانه‌ای نشان دادند. این نشان می‌دهد که نمونه‌های منشوری، با هندسه باریک‌تر و تمایل کمتر به رفتار ترد، برای آزمایش UCS مناسب‌تر تلقی می‌شوند. این نتایج می‌تواند دقت ارزیابی خواص مکانیکی مواد تونل‌زنی را بهبود بخشد، به ویژه آنهایی که در ساخت و سازهای زیرسطحی در جاده‌ها و بزرگراه‌های شهری استفاده می‌شوند.

کلمات کلیدی: اثر شکل و اندازه، مقاومت فشاری تک محوری، مدول الاستیک، سرعت موج فشار، ناهمگنی، مواد شکننده و انعطاف‌پذیر.